Influence of surface properties of the titanium dioxide porous films on the characteristics of solar cells*

T. M. Serikov,[a] N. Kh. Ibrayev,[a] N. Nuraje,[b] S. V. Savilov,[c] and V. V. Lunin[c]*

[a]*Institute of Molecular Nanophotonics, E. A. Buketov Karaganda State University, 28a ul. Universitetskaya, 100026 Karaganda, Republic of Kazakhstan. E-mail: serikov-timur@mail.ru*
[b]*Department of Chemical Engineering, Texas Tech University, PO Box 43121, Lubbock, TX, 79409-3121, USA. E-mail: nurxat.nuraje@ttu.edu*
[c]*Department of Chemistry, M. V. Lomonosov Moscow State University, Build. 3, 1 Leninskie Gory, 1199912 Moscow, Russian Federation. E-mail: savilov@mail.ru*

Porous films formed by cylindrical geometrically anisotropic fragments of TiO_2 have been produced by electrochemical anodization of titanium. The specific surface area and pore volume of the samples were determined by the BET method. It is shown that the samples have a bimodal pore-size distribution with maxima depending on the anodization voltage: by increase in voltage the inner diameter of the cylindrical pores grows, which leads to a decrease in the specific surface area. Dye sensitized solar cells were assembled on the basis of the obtained materials to study the effect of certain characteristics on the efficiency of solar energy conversion. The electrical transport properties of the films were studied by impedance spectroscopy.

Key words: specific surface area, titanium dioxide nanotubes, efficiency of solar cells, electron transport properties.

Dye-sensitized solar cells (DSSC) based on oxide semiconductors are intensively studied as a promising alternative to silicon solar cells due to their commercial availability and ease of manufacture.[1—3] One of the key components of the DSSC is a semiconductor photoelectrode with adsorbed dye. It is known that the amount of light absorbed by a photovoltaic cell directly depends on the concentration of the dye. It can be assumed that an increase in the specific surface area of the oxide layer would allow more dye molecules to be adsorbed and lead to an increase in the sunlight absorption and an increase in the number of charge carriers in the semiconductor.

At present, nanostructured TiO_2 is the most widely used photoelectrode in DSSC.[4—6] It is possible to obtain zero-, one- and two-dimensional nanostructures of titanium dioxide using different synthetic approaches.[7—13] Porous films formed by tubular formations of TiO_2 have a number of advantages. The films formed by TiO_2 nanoparticles are interesting for the possibility of three-dimensional electron transport. The peculiarities of agglomeration of titanium dioxide nanoparticles during annealing significantly influences the possibilities of electron transitions between them. In particular, non-intensive chemical binding leads to a decrease in the efficiency of electron transport. Therefore, when porous films formed by the cylindrical geometrically anisotropic TiO_2 fragments are used, a preferential electron transport along their walls can be expected in DSSC. This reduces the time of transfer from the generation centers of charge carriers to the current collectors, and, if optimized, will achieve a reduction in the number of defects.[14] One of the most common methods for the fabrication of such materials is the electrochemical anodization of titanium in the fluorine-containing electrolyte.[15] The film properties, for example, the specific surface area, can be influenced during the synthesis by various factor, among which, are the anodization voltage, temperature, pH, ratio of electrolyte components, *etc*. Attempts to achieve an increase in the specific surface area of tubular TiO_2 nanostructures by varying the conditions of synthesis are described in many publications. In particular, the specific surface area can be increased[16] to 116 $m^2\ g^{-1}$ by treating the nanostructures with titanium chloride at a temperature >100 °C. Similar results were obtained by other authors.[17—20] At present, the maximum efficiency, equal to 11.2%, has been achieved[21] in DSSC by using 25 nm TiO_2 nanoparticles. In respect to the efficiency of solar cells, tubular nanostructures of titanium dioxide are infe-

* Dedicated to Academician of the Russian Academy of Sciences S. Z. Sagdeev on the occasion of his 75th birthday.

Published in Russian in *Izvestiya Akademii Nauk. Seriya Khimicheskaya,* No. 4, pp. 0614—0621, April, 2017.

rior to nanoparticles.[22] One of the reasons is that the specific surface area of films from nanoparticles is significantly higher than that of other TiO_2 nanostructures films.

Therefore, in recent years, the work has been actively carried out to create the composite materials based on nanoparticles and mesoporous titanium dioxide films synthesized by electrochemical anodization.[23] On the one hand, the use of such structures increases the specific surface area, and on the other hand, the injected electrons can follow a one-dimensional way to the current collectors. In the majority of studies,[24] the synthesis of films by electrochemical anodization was carried out at an anodization voltage of 40—50 V. In this work, we have tried to find out whether the films obtained at an anodization voltage of 20 V have a higher specific surface area than films obtained with higher anodization voltage. In addition, the results for investigation of the electron transport properties of solar photovoltaics are presented.

Experimental

Titanium foil with a thickness of 60 μm was subjected to chemical polishing in the solution composed of H_2SO_4 (60%), HF (25%), $C_3H_5(OH)_3$ (15%), for 10 min according to published procedure.[25] Before an anodization the sample was activated ultrasonically in a 2 *M* HCl solution, and then in acetone to remove impurities.

Ethylene glycol containing 0.5 wt.% of NH_4F and 3 wt.% of H_2O was used as electrolyte. Anodic oxidation of titanium was carried out in the electrochemical cell in potentiostatic mode at temperature of 5—7 °C. Platinum foil served as a cathode. The distance between cathode and anode was 3 cm. Anodization voltage was varied in the range of 20—70 V.

The synthesis of porous titania films consisted of three stages. During the first anodization for 2 h, a film containing hydrolysis by-products was formed on the surface of the titanium foil. This film was removed from the foil surface by sonication in a 1 *M* HCl solution. During the re-anodization for 24 h, cylindrical geometrically anisotropic fragments of TiO_2 were formed, which were then sonicated to remove reaction by-products. TiO_2 was crystallized for 6 h in a muffle oven at a temperature of 773 K. A third anodization step was used to separate the porous film from the titanium foil.[26] The process was carried out at an electrolyte temperature of 343 K and a voltage of 60 V. The end of the process was determined visually from the moment at which the film was completely separated from the foil.

The surface of samples was studied by scanning electron microscopy using MIRA 3LMU (Tescan, Czech Republic) microscope. Acceleration voltage was 30 kV. To carry out the experiment, the separated films of titanium dioxide were fixed to conductive carbon tape to avoid accumulation of charge on the surface.

Specific surface area, pore size distribution, and the pore volume *vs*. their diameter were measured by the method of low-temperature nitrogen sorption using a measuring complex Sorbi-MS (Meta, Russia). The samples were annealed at 100 °C for 2 h in the preparation block SorbiPrep. The pore-size distribution was calculated from the results of low-temperature nitrogen sorption by the BJH model using a AUTOSORB-1C/QMS sorbometer (Quantachrome, USA).

The molecules of Ruthenium dye N719 (di-tetrabutylammonium *cis*-bis(isothiocyanato) bis(2,2′-bipyridyl-4,4′-dicarboxylato) ruthenium(II), Sigma—Aldrich) were adsorbed on the semiconductor film from ethanol solution with a dye concentration of 10^{-4} mol L^{-1} for 18 h. The concentration of dye on the surface of TiO_2 was determined by a change of optical density of dye solution before and after adsorption. Commercially available Iodolyte H30 (Solaronix, Switzeland) was used as an electrolyte in photovoltaic cells. Polymer film Meltonix with a thickness of 25 μm (also from Solaronix) was used as a separator.

The study of the samples with high resolution transmission electron microscopy was performed using a JEM-2100F microscope (JEOL, Japan), equipped with a corrector of spherical aberrations and spectrometer of energy-dispersive spectral analysis. The accelerating voltage was 200 kV. Prior to the test, the sample was dispersed by sonication in ethanol and deposited as a thin layer onto the coated copper grid.

Photoluminescence of the films was measured using an automated spectroscopic-kinetic setup with registration in the photon counting regime at the boiling point of liquid nitrogen (90 K). Nitrogen laser AIL-3 (λ_{gen} = 337 nm, E = 30 μJ, τ_{pulse} = = 10 ns) was used as an excitation source. Before measurements, the sample was placed in an optical cryostat, which was previously evacuated to a residual pressure of $P = 5 \cdot 10^{-4}$ mbar.

Raman spectrum was registered using a HORIBA Jobin Yvon spectrometer, equipped with laser of 532 nm wavelength.

Current-voltage characteristics of photovoltaic cells were measured under illumination with a Xenon lamp with power of 100 mW cm^{-2} (AirMass AM-1.5) using a measurement complex CT50AAA (PET Photo Emission Tech. Inc., USA). The electron transport properties of titanium dioxide films were investigated by measuring the photocurrent and impedance of an electrochemical cell by electrochemical impedance spectroscopy under standard simulated solar radiation from an AM-1.5 lamp with power of 100 mW cm^{-2} using Z-500PRO (Elins, Russia) spectrometer. The amplitude of applied sinusoidal signal was 20 mV, the frequency was varied from 1 MHz to 100 mHz.

Results and Discussion

Electrochemical anodization of titanium foil with careful control of external conditions made it possible to obtain nanostructured porous TiO_2 films. The microphotography of the surface of the films separated from titanium foil (Fig. 1) exhibits good formed films from densely packed cylindrical geometrically anisotropic titanium dioxide fragments located perpendicular to the plane of the foil. The porous structure of the film and the dimensions of the individual channels, which are of 130 nm, are clearly visible. The surface of TiO_2. films contains only small number of defects, and the films themselves have a clearly marked channel along the entire length.

The results of the study of the films by the method of high resolution transmission electron microscopy are presented in Fig. 2.

Before thermal treatment, TiO_2 has an amorphous structure. Crystallization occurs during thermal annealing of the sample starting at a temperature of 553 K. At 773 K, the amorphous phase transfers into the crystalline phase

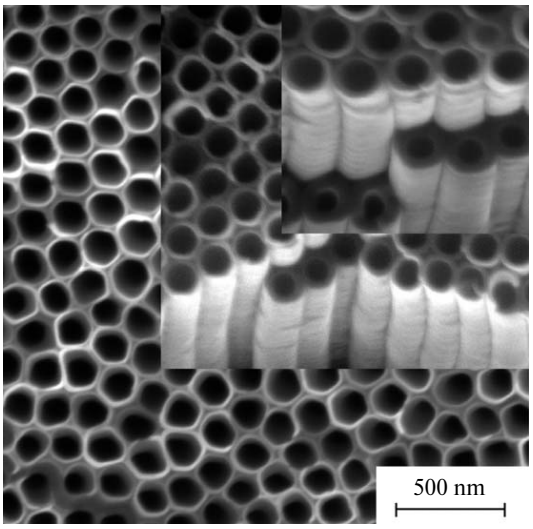

Fig. 1. Microimage of titania film surface, obtained by electrochemical anodization.

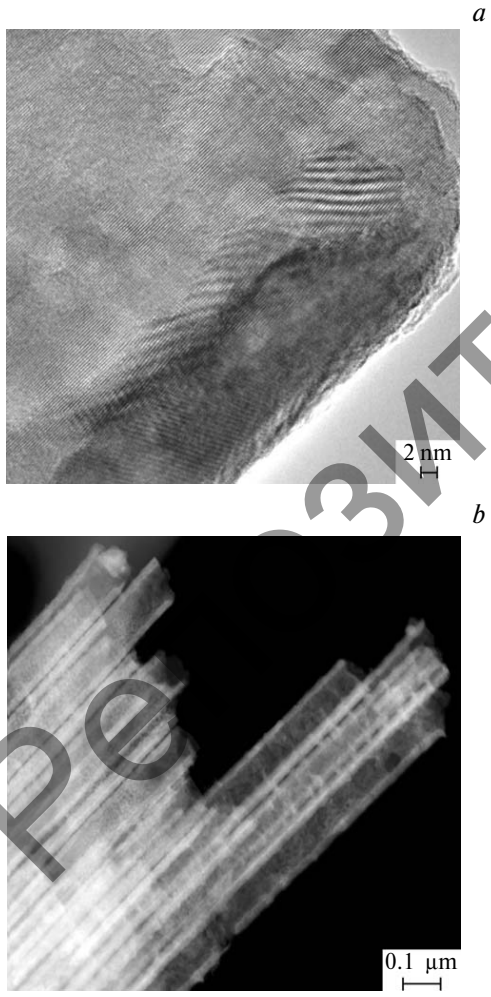

Fig. 2. High resolution microimage of titania films at different magnification.

with the anatase structure. With further annealing up to 1273 K, the anatase structure is completely rearranged to the rutile phase.[27]

The photoluminescence and Raman spectra of TiO_2 film obtained at an anodization voltage of 50 V and subjected to thermal annealing at a temperature of 773 K are presented in Fig. 3.

When the samples are excited in the UV region of the spectrum, a broad luminescence band with maxima at 510 and 540 nm is observed in the wavelength range of 400—800 nm (see Fig. 3, *a*). By lowering the substrate temperature to 90 K, the luminescence intensity is increased. Registered photoluminescence spectrum agrees with the published earlier spectrum and is characteristic of the anatase structure.[28]

The nature of this luminescence is associated with defects located in the near-surface region of crystallites.[27] Using the approximation by Gaussian functions, the luminescence spectra were divided into components as it is shown in Fig. 3, *a*. The results of the approximation show that the observed luminescence spectra contain three bands with maxima at 510, 540, and 600 nm. The registered

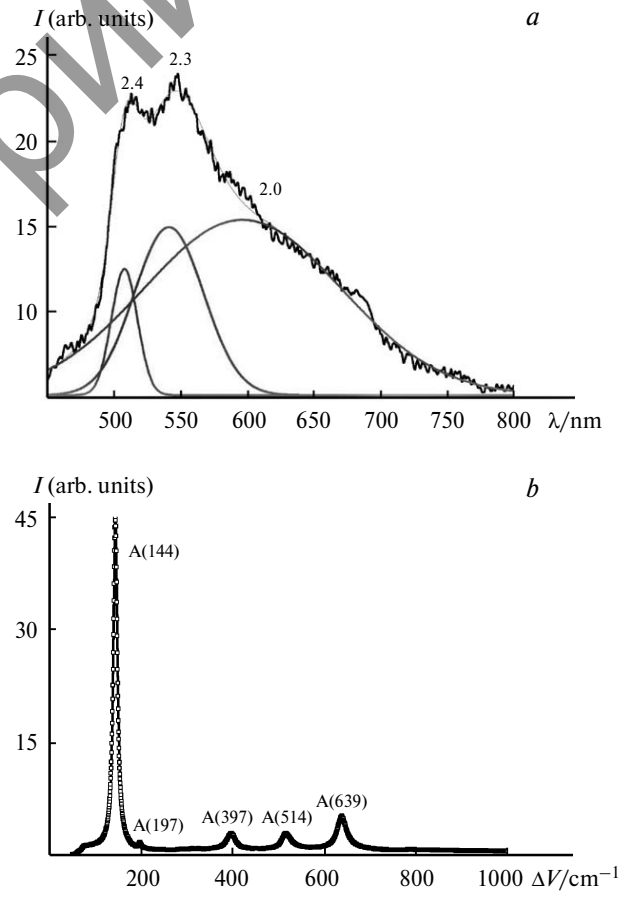

Fig. 3. Luminescence (*a*) and Raman (*b*) spectra of titanium dioxide films; the numbers on the curves are the energy of the glow (eV).

spectra correlate well with the literature data.[29] The luminescence of the anatase structure of nanocrystalline titanium dioxide is associated with three possible defect states: self-trapped excitons STE, Ti^{3+}/F, and F^+.[29]

Raman spectrum of the same TiO_2 film is represented in Fig. 3, *b*. The features are also characteristic of anatase structure. It is known [30] that anatase exhibit five active Raman modes: $A_{1g} + B_{1g}$ (2) 514 cm^{-1}; B_{1g} (1) 397 cm^{-1}; E_g (1) 144 cm^{-1}; E_g (2) 197 cm^{-1}; E_g (3) 639 cm^{-1}. These modes correspond to irreducible representations of symmetry groups A_{1g}, $2B_{1g}$, and $3E_g$.

Similar data were obtained for both photoluminescence and Raman spectroscopy for films synthesized at anodization voltage of 20 and 70 V. Thus, the results of measuring the photoluminescence and Raman spectra indicate that under the conditions selected for the synthesis of porous TiO_2 films, the phase composition of geometrically anisotropic fragments corresponds to the anatase structure.

The specific surface area of semiconductor films is one of the critical characteristics for DSSC. The surface concentration of the adsorbed dye and, ultimately, the number of electrons photoinjected into the conduction band of the semiconductor depend on this parameter. The influence of the voltage and duration of anodization on the surface properties of TiO_2 films was studied to determine the optimum conditions for the production of porous films. The results of measurements of the specific surface area of the samples, calculated by the Brunauer—Emmett—Teller equation (BET), are presented in Table 1.

The number of pores per surface unit was estimated by statistical processing of microimages recorded by scanning electron microscopy. It follows from the obtained data that as the anodization voltage increases, the internal diameter and the length of the pores increase. The surface concentration decreases due to increasing internal pore diameter, which leads to a drop in the specific surface area and pore volume. These results correlate well with the literature data.[31] Calculation of the pore-size distribution is performed based on the isotherm of nitrogen adsorption and desorption using on the Barrett—Joyner—Halenda (BJH) model (Fig. 4).

According to the IUPAC classification of porous systems,[32] the samples have meso- and macroporous structure. However, as the anodization voltage increases, the number of mesopores decreases. The presence of pores with diameters <40 nm is associated, obviously, with the voids formed between the anisotropic fragments of titanium dioxide during their packing, which is clearly seen in the pictures recorded by transmission electron microscopy.

The effect of anodization duration on the pore length of titanium dioxide films was studied using the samples synthesized at an anodization voltage of 50 V. The duration of the second anodization step varied from 1 to 30 h.

As it can be seen from Fig. 5, the pore length increases linearly with time for 24 h from the start of anodization to reach a value of ~36 мм and die away thereafter. The growth of pores is terminated when an equilibrium is attained between the rate of dissolution of the oxide in the mouth of the pores and the rate of movement of the barrier layer inside the metal.

The samples obtained at the anodization voltage of 20, 50, and 70 V were selected to study the effect of the specific surface area of the films on the efficiency of solar cells. The cells were assembled using these samples and the current-voltage characteristics of the cells were measured (Fig. 6).

It is evident that in a cell based on the film obtained at the anodization voltage of 20 V and having the largest specific surface area, the current density is higher than for the films synthesized at voltages of 50 and 70 V. It is known that the value of the cell open circuit voltage is determined by the nature of the used materials, and the current density is determined by the number of dye molecules adsorbed.

The surface concentration of the dye on the TiO_2 film was estimated from the change in the optical density of the alcoholic solution of the dye measured before and after adsorption. As it is clear from Fig. 7, the optical density of the solution decreases with increasing sorption duration that indicates the introduction of the dye molecules into the pores of the films. For the film synthesized at the

Table 1. Characteristics* of the films formed by cylindrical geometrically anisotropic fragments of TiO_2 obtained at various anodization voltages

Voltage/V	L/μm	d_{av}/nm	Specific surface area, $S_{BET}/m^2\ g^{-1}$	Concentration of pores · 10^{-9}/number cm^{-2}	Total pore volume, $V_p/cm^3\ g^{-1}$
20	17.1	55	71	25.0	0.200
30	22.0	70	68	22.0	0.155
40	27.0	90	65	11.0	0.128
50	36.0	110	63	6.0	0.112
60	37.0	140	61	2.5	0.106
70	40.0	150	59	0.5	0.102

* L and d_{av} are the length and diameter of pores, respectively.

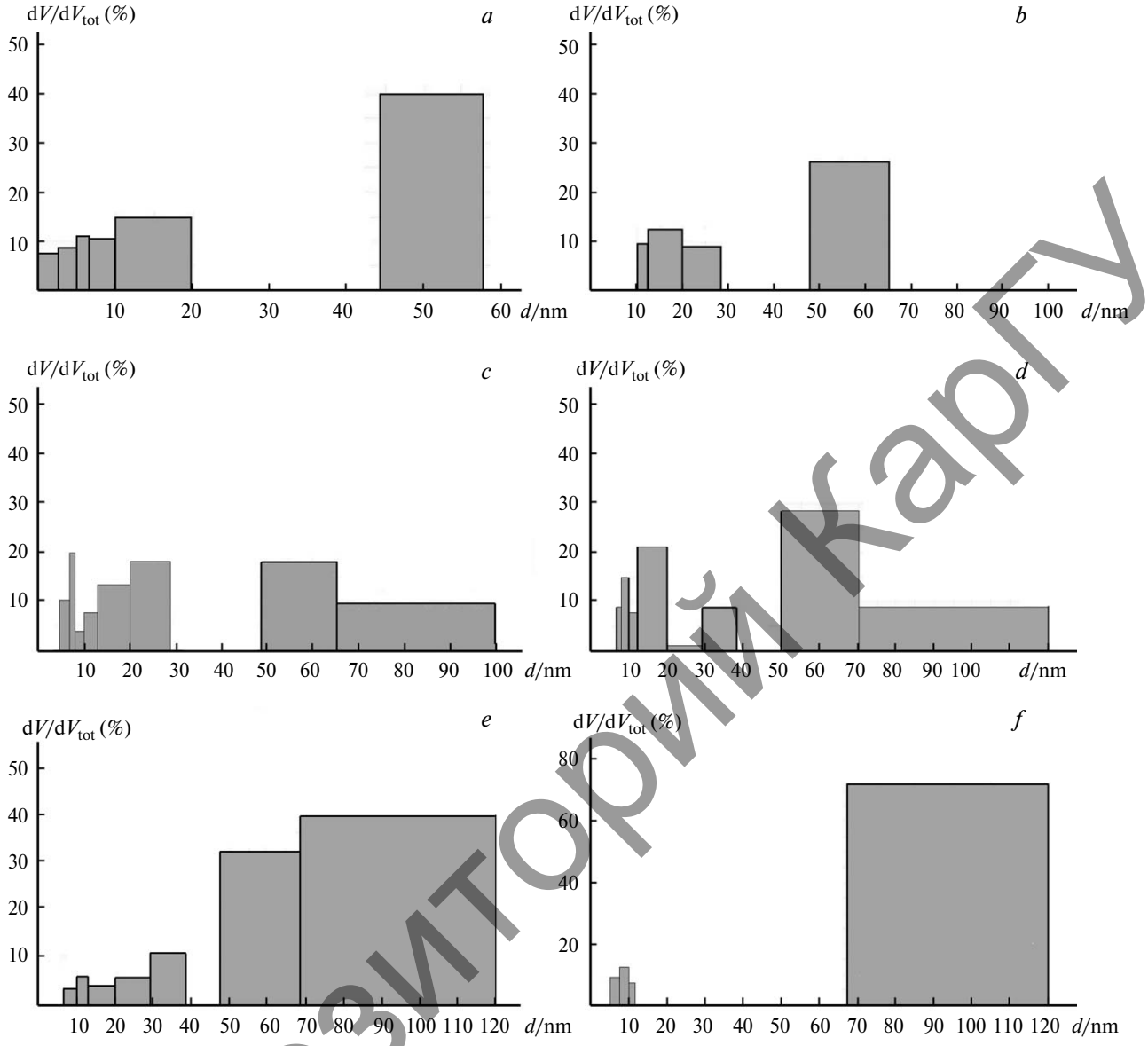

Fig. 4. Pore-size distribution of TiO_2 at different anodization voltages: 20 (*a*), 30 (*b*), 40 (*c*), 50 (*d*), 60 (*e*), and 70 V (*f*); V_{tot} is the total pore volume.

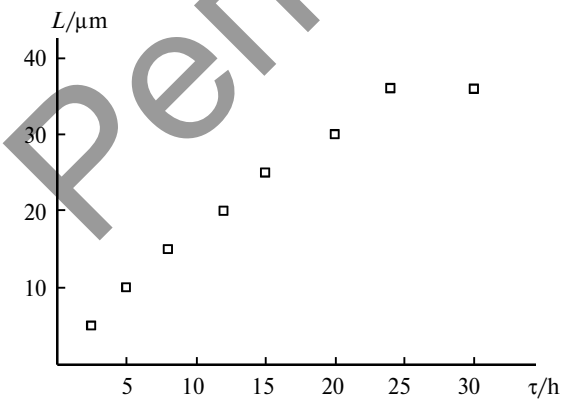

Fig. 5. Dependence of pore length (L) on the duration of second anodization step (τ).

anodization voltage of 20 V, the highest sorption capacity is observed. This is confirmed by the data of the BET specific surface area measurements. The optimum duration of sorption was 18 h, since its further increase did not lead to a decrease in the optical density of the solution.

The surface concentration of dye molecules adsorbed by porous TiO_2 films (C) was determined according to equation:

$$C = (N_A C_0 V/S)(1 - D_2/D_1),$$

where N_A is the Avogadro constant; C_0 is the initial dye concentration in the ethanol ($1 \cdot 10^{-4}$ mol L^{-1}); V is the solution volume; S is the surface area of the adsorbent; D_1 and D_2 are the solution optical densities before and

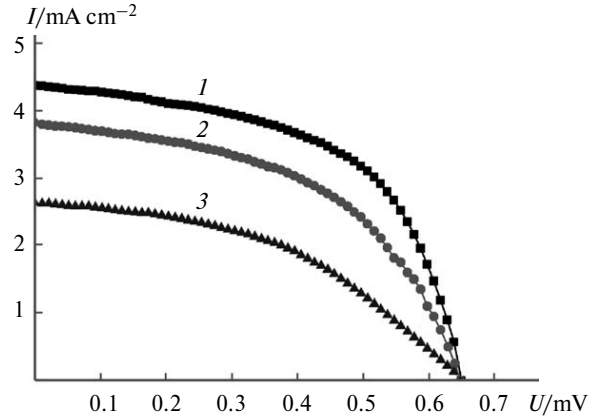

Fig. 6. Current-voltage characteristics of solar cells on the basis of films obtained at anodization voltage of 20 (*1*), 50 (*2*), and 70 V (*3*).

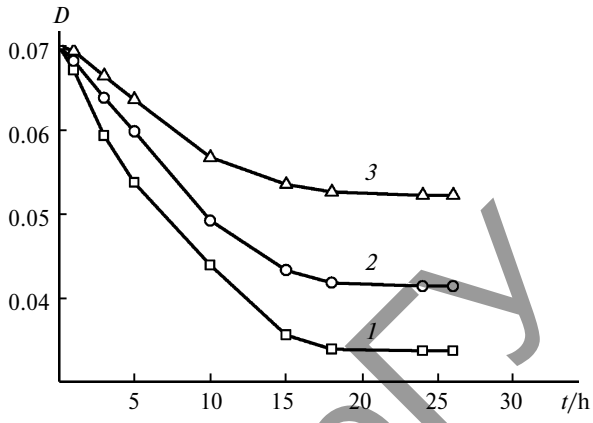

Fig. 7. Dependence of optical density (*D*) of dye N719 on the duration of sorption (*t*) for the films obtained at anodization voltage of 20 (*1*), 50 (*2*), and 70 V (*3*).

after adsorption, respectively. The results of the calculation are presented below.

Anodization voltage/V	$C \cdot 10^{-16}$/mol cm^{-2}
20	25.1
50	19.7
70	12.0

Thus, it is demonstrated that the larger the specific surface area of the films is, the more dye molecules can be sorbed into its pores. This leads, in turn, to an increase in the number of electrons injected into the semiconductor by the action of solar radiation and an increase in the cell current. The main parameters of the photovoltaic elements were determined on the basis of obtained experimental dependencies (Table 2). The parameters were calculated using the program package IV-Measurement in accordance with known methods.[33] The presented values of the solar cells efficiency are not higher than the data in the literature, but they can reliably reveal all the necessary dependencies.

It is clear from the data in Table 2 that the cell based on the TiO_2 film obtained by anodization at 20 V has the highest efficiency. The resistance R_p increases with the anodization voltage. For a real solar cell, this value is composed of series-connected resistances, the values of which depend on the quality of the interlayer contacts, and the resistance R_{sh} reflects possible channels of the current leakage. In an ideal solar cell $R_p \to 0$, and $R_{sh} \to \infty$.

One of the most widely used methods for the investigation of the electrical transport properties of solar cells, which depend primarily on the oxide semiconductor photoelectrode, is the measurement of the electrical impedance.[34] The impedance parametric plots in the Nyquist coordinates for the DSSC based on TiO_2 films obtained at voltages of 20, 50, and 70 V are presented in Fig. 8. The results of impedance measurements were analyzed according to the diffusion-recombination model under the assumption of the equivalence of the chains considered and illustrated in Fig. 7.[35] Experimental data were processed with the help of the software package EIS-analyzer.[36]

According to the technique described earlier[37] based on the recorded impedance spectra for the photocells, a number of parameters were calculated. Among these: the effective diffusion coefficient of the electrons D_{eff}, the effective recombination rate of the electron k_{eff}, the effective lifetime of the electron τ_{eff}, the electron transport resistance in the titania film R_w, and the charge transfer resistance associated with recombination of the electrons R_k. The results are presented in Table 3.

It is known,[38] that in the case when the resulting impedance experimental arc of parametric plot is a part of

Table 2. Electrophysical parameters* of solar cells

Voltage/V		Short circuit current/mA cm^{-2}	Fill factor, FF	R_p	R_{sh}	Efficiency (%)
of anodization	open circuit			Ohm		
20	0.65	4.37	0.55	39	1684	1.65
50	0.64	3.82	0.52	44	1813	1.47
70	0.64	2.64	0.44	241	2118	1.08

* R_p and R_{sh} are the resistances of the cell, included in chain in series and parallel, respectively.

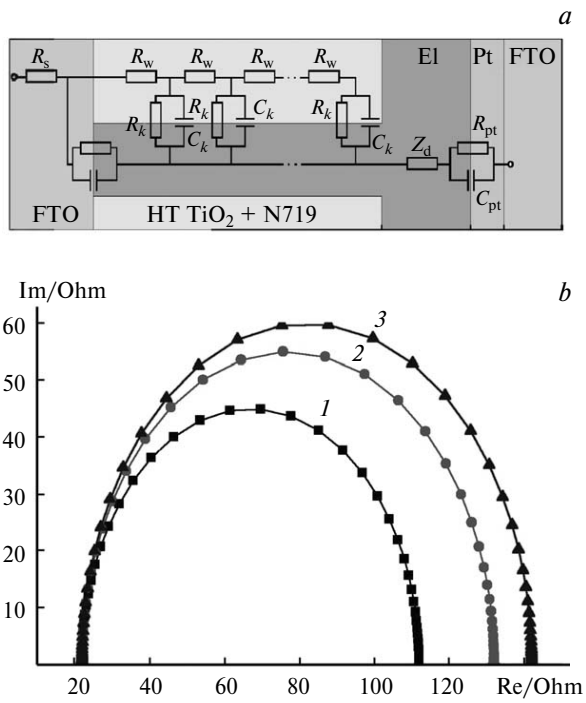

Fig. 8. Model of processes in a solar cell (*a*) and impedance parametric plots in the Nyquist coordinates for the DSSC, obtained at 20 (*1*), 50 (*2*), and 70 V (*3*); R_s is the series resistance, taking into account the resistance of the interface FTO/TiO_2; R_w (R_{wire}) is the resistance to electron transport in the film of titanium dioxide; R_k is the charge transfer resistance associated with the recombination of an electron that arises at interface between electrolyte (El) and titania film; C_k is the capacitance at the semiconductor/electrolyte interface; C_{pt} is the interfacial capacitance at the interface of counter electrode/electrolyte; FTO is the fluorine doped tin oxide; R_{pt} is the charge transfer resistance at the interface of counter electrode/electrolyte; Z_d is the total resistance to redox processes diffusion in the electrolyte.

a regular circle, the values of R_k are much larger than the values of R_w. Experimental data provide evidence that with an increase in the anodization voltage, the values of R_w increase insignificantly, while R_k and τ_{eff} are at minimum in the cell with the largest surface area. This can be explained as due to the fact that as the surface area of the films increases, the TiO_2/electrolyte interface increases and the number of injected electrons increases, which undoubtedly increases the recombination rate. The obtained results are in good agreement with the well-known model.[35]

Thus, titanium dioxide films consisting of perpendicularly arranged tubular formations were obtained by the electrochemical anodization of titanium foil. Electron microscopic examination indicated that with increasing anodization voltage, the internal diameter and the length of the pores increase. Mathematical interpretation of the results of experiments on low-temperature nitrogen adsorption based on the BET and BJH models suggests that the films obtained at the anodization voltage of 20 V have the highest specific surface area. This fact is confirmed by electron microscopic studies. It is shown that the pore-size distribution is bimodal with maxima that also depend on the anodization voltage. The dye sensitized solar photocells are assembled on the basis of the obtained films, and their photovoltaic and electro transport properties are studied. It is found that the best parameters are obtained for the cell based on the porous TiO_2 film prepared at the anodization voltage of 20 V.

At the same time, the efficiencies of the investigated solar cells, despite the one-dimensional transport of electrons in them, remain low in comparison with the cells based on TiO_2 nanoparticles, since the specific surface area of nanoparticles is much higher. In this respect, to achieve higher efficiency for DSSC, it is desirable to create new composite materials based on nanoparticles, nanotubes, and TiO_2 nanorods. In such structures, the film would show higher specific surface area due to the use of nanoparticles. This in turn would result in higher concentrations of photoinjected electrons migrating along one-dimensional nanostructures and rapidly reaching the removable electrodes.

The authors are grateful to A. V. Egorov for helping with transmission electron microscopic study. The investigation of materials was performed using the equipment acquired under the Development Program of M. V. Lomonosov Moscow State University.

This study was financially supported by the Russian Science Foundation (Project No. 14-03-00072) and Com-

Table 3. Electro transport parameters* of the solar cell obtained at different voltages

Anodization voltage/V	$D_{eff} \cdot 10^4$ /cm^2 s^{-1}	k_{eff}	τ_{eff}	R_k	R_w	Con/Ohm cm s^{-1}	L/cm
		s^{-1}		Ohm			
20	2.4	83	0.012	80	10.0	11.3	0.00171
50	9.4	73	0.013	112	11.2	29.4	0.00360
70	9.6	60	0.016	121	12.8	29.0	0.00400

* k_{eff} is the effective recombination rate, R_k is charge transfer resistance associated with the recombination of an electron, Con = $R_k L k_{eff}$, L is the thickness of TiO_2 semiconductor.

mittee of Science of the Ministry of Education of the Republic of Kazakhstan (Project No. 0088/PTF).

References

1. B. O´Regan, M. Gratzel, *Nature*, 1991, **353**, 737.
2. S. Ito, T. N. Murakami, P. Comtel, *Thin Solid Films*, 2008, **516**, 4613.
3. J. Lee, K. Hong, K. Shin, J. Y. Jho, *J. Ind. Eng. Chem.,* 2012, **18**, 19.
4. T. Ma, M. Akiyama, E. Abe, I. Imai, *Nano Lett*., 2005, **5**, 2543.
5. E. Crossland, M. Kamperman, M. Nedelcu, *Nano Lett.*, **9**, 2807.
6. S. Guldin, S. Hьttner, M. Kolle, M. E. Welland, *Nano Lett*., 2010, **10**, 2303.
7. J. Yang, S. Mei, Ferreira, *Mater. Sci. Eng.: C*, 2001, **15**, 183.
8. X. Yan, J. Kang, L. Gao, L. Xiong, *Appl. Surface Sci.,* 2013, **265**, 778.
9. S. Sahni, S. Bhaskar, *Mater. Sci. Eng.: A*, 2007, **452**, 758.
10. H. O. Pierson, *Nature*, 1992, **43**, 235.
11. S. H. Nam, J. S. Hyun, J. H. Boo, *Mater. Res. Bull.*, 2012, **47**, 2717.
12. Y. Zhu, H. Li, Y. Koltypin, Y. Hacohen, A. Gedanken, *Chem. Commun*., 2001, **24**, 2616—2617.
13. X. Wu, Q. Z. Jiang, Z. F. Ma, M. Fu, W. F. Shangguan, *Solid State Commun*., 2005, **136**, 513.
14. D. Mukul, H. Hongshan, *Scanning Electron Microscopy*, 2012, **27**, 537.
15. D. Gong, C. A. Grimes, O. K. Varghese, W. Hu, R. S. Singh, *J. Mater. Res.*, 2001, **16**, 3331.
16. H. Wang, H. Li, J. Wang, *Electrochim. Acta*, 2014, **137**, 744.
17. N. Pugazhenthirana, S. Murugesana, S. Anandan, *J. Hazardous Mater.*, 2013, **263**, 541.
18. O. P. Ferreira, A. G. Souza, J. M. Filho, O. L. Alves, *J. Braz. Chem. Soc*., 2006, **17**, 2.
19. T. Kasuga, M. Hiramatsu, A. Hoson, T. Sekino, K. Niihara, *Langmuir*, 1998, **14**, 3160.
20. B. Abidaa, L. Chirchia, S. Barantonb, A. Ghorbela, *Appl. Catal. B: Environmental*, 2011, **106**, 609.
21. Y. Chiba, A. Islam, Y. Watanabe, *Jpn J. Appl. Phys.*, 2006, **25**, 638.
22. A. J. Frank, N. Kopidakis, J. Lagemaat, *Coord. Chem. Rev*., 2004, **248**, 1165.
23. J. Choi, G. Kang, T. Park, *J. Chem. Mater.*, 2015, **5**, 1.
24. J. Zhang, S. Li, H. Ding, *J. Power Sources*, 2014, **247**, 807.
25. D. I. Petukhov, A. A. Eliseev, I. V. Kolesnik, K. S. Napolskii, *J. Porous Mater.*, 2011, **19**, 71.
26. J. Lin, J. Chen, X. Chen, *Electrochem. Commun.*, 2010, **12**, 1062.
27. H. Zhang, M. Zhou, Q. Fu, B. Lei, W. Lin, H. Guo, M. Wu, Y. Lei, *Nanotechnology*, 2014, **25**, 275603.
28. X. Wang, Z. Feng, J. Shi, *Phys. Chem. Chem. Phys.*, 2010, **12**, 7083.
29. C. Mercado, Z. Seeley, A. Bandyopadhyay, S. Bose, J. L. Mchale, *ACS Appl. Mater. Interfaces*, 2011, **3**, 2281.
30. T. Ohsaka, F. Izumi, Y. Fujiki, *J. Raman Spectrosc.*, 1978, **7**, 321.
31. A. N. Morozov. A. I. Mikhailichenko, *Uspekhi v khimii i khimicheskoi tekhnologii* [*Rev. in Chem. and Chem. Technology*], 2012, **11**, 30 (in Russian).
32. *IUPAC Manual of Symbols and Terminology, Pure Appl. Chem.*, 1972, **31**, 578.
33. K. Chawla, 2011; www.photoemission.com.
34. J. Bisquert, F. Fabregat-Santiago, *Impedance Spectroscopy: A General Introduction and Application to Dye—Sensitized Solar Cells*, CRC Press, Boca Raton, 2010, 457.
35. R. Kern, R. Sastrawan, J. Ferber, R. Stangl, J. Luther, *Electrochim. Acta*, 2002, **47**, 4213.
36. A. S. Bondarenko, G. A. Ragoisha. *Inverse problem in potentiodynamic electrochemical impedance spectroscopy*, in *Progress in Chemometrics Research*, Ed. A. L. Pomerantsev, *Nova Sci. Publ.*, New York, 2005, 89-102.
37. M. Adachi, M. Sakamoto, J. Jiu, Y. Ogata, S. Isoda, *J. Phys. Chem. B.*, 2006, **110**, 13872.
38. F. Fabregat-Santiago, J. Bisquert, G. Garcia-Belmonte, G. Boschloo, A. Hagfeldt, *Solar Energy Mater. Solar Cells*, 2005, **87**, 117.

Received August 7, 2016;
in revised form December 2, 2016